



Estuary rejuvenation in response to sea level rise: an example from Tairua Estuary, New Zealand

Z. Cathy Liu¹ · W. P. de Lange¹ · K. R. Bryan¹

Received: 27 February 2019 / Accepted: 24 September 2019 / Published online: 24 October 2019
© Springer-Verlag GmbH Germany, part of Springer Nature 2019

Abstract

Under stable sea level conditions, estuaries tend to accumulate sediment resulting in changes that can be conceptualised as a progression from a juvenile system to maturity. Sea level rise results in an increase in accommodation space within the estuary that can effectively reverse the progression towards maturity. This effect was investigated for Tairua Estuary, New Zealand, using a set of MIKE 21 HD (hydrodynamic) and MIKE 21 ST (sediment transport) numerical models forced by tides, wind and fluvial discharges. A range of scenarios of sea level rise and changing fluvial inputs were simulated. The simulation results predicted a general trend of increasing tidal range with sea level rise, which was partially offset by higher fluvial discharges within high fluvial input scenarios. Under present conditions, the estuary is ebb-dominated with predominantly fluvial inputs, but with increasing sea level, the estuary becomes increasingly flood-dominant and the transition from fluvial to marine sediments within the estuary progressively moves landward. If the sediment supply increases in tandem with the accommodation space, the result would be no significant change to the estuary's hydrodynamics and sediment transport patterns. Under present conditions, observations and modelling indicate that sediment is exported by ebb-dominant conditions, suggesting a capacity to compensate for increasing accommodation space. However, modelling indicates a sediment deficit at higher projected sea levels, resulting in sediment being scavenged from the seaward margin of the sandy barrier spit enclosing the estuary. Scavenging would increase the coastal erosion hazard for the residents of the barrier spit. This situation does not arise if the rate of increase in accommodation space remains below the annual fluvial sediment supply. Ultimately, our results show the importance of considering catchment-derived sediment supply and morphological complexity, when predicting how the changing hydrodynamics modulate the interplay between sediment stored within the estuary and the open coast, and determining the fate of the coast during sea level rise.

Introduction

Low-lying coastal areas are particularly vulnerable to sea level rise (SLR) (Nicholls et al. 1999; Cahoon et al. 2006), and creating useful adaptation plans requires a robust understanding of the change in hazard and risk across the coastal zone. Within estuarine systems, changes in inundation regimes are dependent on the ability of fringing intertidal land to trap enough sediment to keep pace with SLR (van Maanen et al. 2013; Kirwan et al. 2016). If insufficient sediment is available, the estuary may “roll-over” or migrate landward while retaining its general form (Townend and Pethick 2002). In contrast, if sufficient sediment is available, increased

accommodation space results in accretion and potentially infilling of the estuary (Kieft et al. 2011; Lorenzo-Trueba and Ashton 2014).

Sediment may be supplied to the estuary by fluvial transport from a terrestrial source, or by a combination of tidal and wave-induced transport from a marine or coastal source, or formed in situ by biogenic processes (Dalrymple et al. 1992; Masselink et al. 2011). Suspended sediment discharge from New Zealand rivers is largely dependent on precipitation within the catchment, and bedload sediment discharge is assumed to follow the same dependency (Hicks et al. 2011). On the open coast, sediment supply from estuaries and cliffs is needed to compensate for sediment removed from beaches as a consequence of increased erosion due to potential and observed changes in storminess (e.g. Hemer et al. 2010; Godoi et al. 2016). This suggests that the response to sea level rise may be mediated by other climatic changes that affect sediment availability (viz. Palmer et al. 2019). However, the response of the estuarine system is likely to be highly localised,

✉ K. R. Bryan
karin.bryan@waikato.ac.nz

¹ School of Science, University of Waikato, Hamilton, New Zealand

depending on, for example, the catchment properties, the underlying geology, the tidal range and the fluvial discharge.

Here, we explore the effect of sea level rise on a barrier-enclosed estuary on the North Island of New Zealand using numerical modelling techniques. The focus of this study is on changes to hydrodynamic processes within the estuary and the consequences for sediment transport.

The study was conducted in the Tairua Estuary located on the east coast of the Coromandel Peninsula, North Island of New Zealand (Fig. 1). The estuary is separated from the open ocean to the east by the 2.7-km-long Pauanui sand spit to the south and the 1.2-km-long Ocean Beach tombolo to the north (Hume and Gibb 1987). Paku Mountain anchors the southern end of the Ocean Beach tombolo and constrains the northern boundary of the tidal inlet.

The Tairua catchment is steep and mountainous, rising to a maximum height of 830 m above mean sea level (MSL) at the headwaters of the Tairua River. The total catchment area is 282 km², with almost half the catchment covered by indigenous forest (Hume and Gibb 1987). Tairua Estuary is

characterised by a shallow narrow basin, narrow estuary mouth and relatively small fluvial input except during intense rainfall events. The tidal prism reported by Bell (1994) for October–November 1983 varied from 4.0 Mm³ (neap) to 6.1 Mm³ (spring), while Barnett Consultants determined a spring tide prism of 5.0 Mm³ in 1991 (Liu 2014). The ratio of total estuary volume to tidal prism is low (Hume and Herdendorf 1988); thus, the estuary has a relatively short tidal flushing time. As a consequence, it varies between category C (fluvially dominated) and category E (tidally dominated) estuarine conditions following the classification of Hume et al. (2007).

The estuary is largely infilled with Holocene sandy sediment, with evidence for several phases of deposition, potentially linked to fluctuating sea levels up to 1.5 m above present (Kennedy 2008), and Holocene marine terraces at approximately 1.3 m and 5 m above MSL (Hayward and Morley 2014). Sediment texture varies within the estuary from very coarse to coarse sand in the deeper tidal channels, to fine sand on the upper tidal flats (Felsing and Giles 2011). Sediment

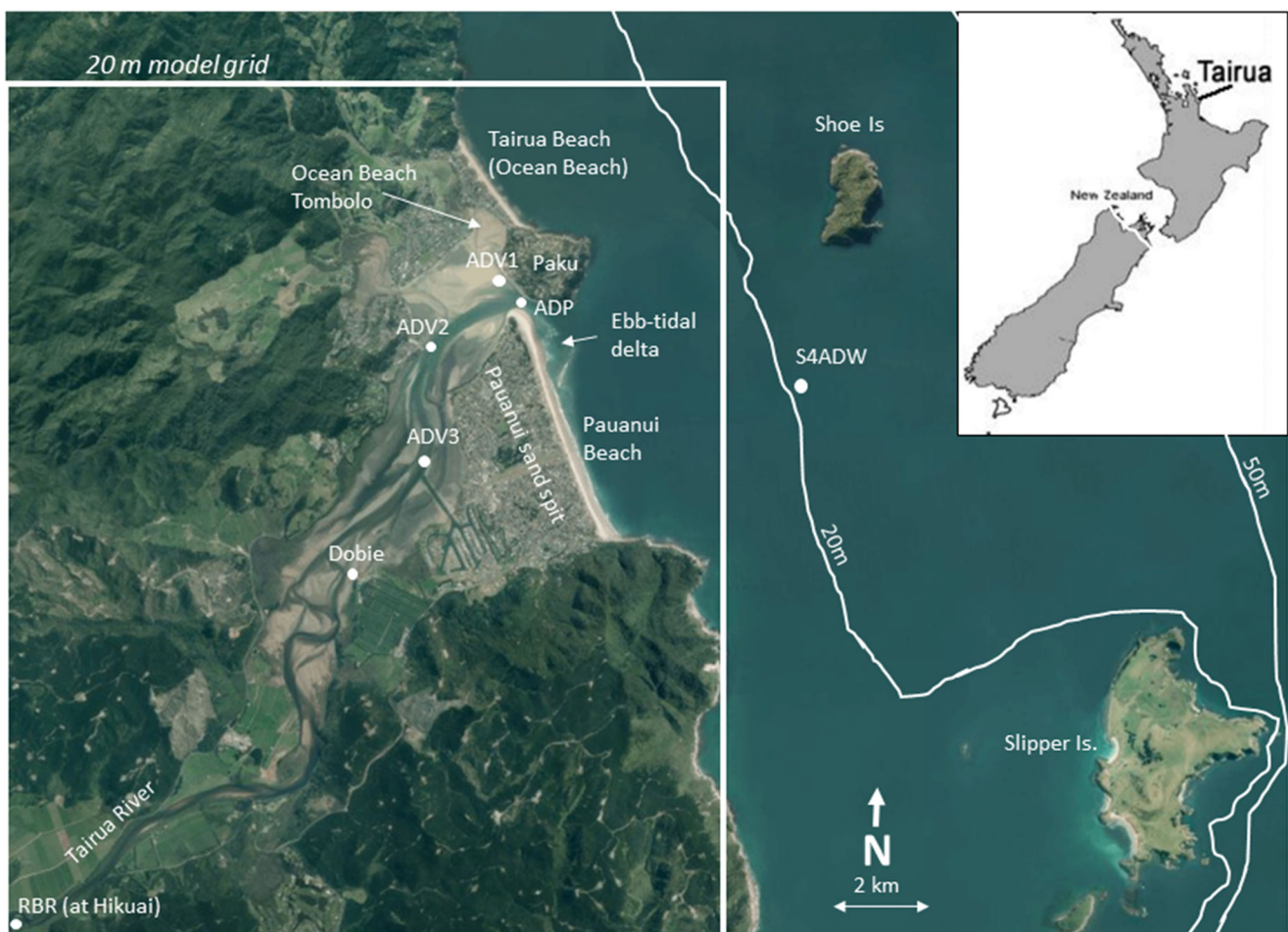


Fig. 1 Location map of Tairua Estuary showing the positions occupied by instruments during calibration and validation field deployments, and the boundary of the higher resolution numerical model used by the study (the

low-resolution boundary matches the extent of the mapped area to the north and west and extends 3.5 km southward). Background image is an aerial photograph provided by Land Information New Zealand

deposited with the estuary is assumed to be mostly derived from fluvial sources at a rate of $10,000 \pm 2000 \text{ m}^3 \text{ year}^{-1}$ (Gibb and Aburn 1986). Sedimentation rates have been estimated as 6 mm year^{-1} for the intertidal flats, increasing to 10–19 mm year^{-1} close to fluvial sources, and up to 22 mm year^{-1} at the entrance to the estuary (Hume and Gibb 1987).

The high rates of sedimentation at the entrance appear to be derived from marine-sourced sediment (Liu 2014). Tairua and Pauanui beaches on the seaward margins of the barriers enclosing the estuary (Fig. 1) are comprised of medium to coarse sand (Gibb and Aburn 1986; Smith and Bryan 2007). The seabed of the offshore embayment is composed of sandy sediment; however, grain size varies appreciably (Liu 2014).

The specific objectives of the study were to determine the potential effects of sea level rise and fluvial discharge changes on (1) the tidal amplitude and asymmetry, (2) the extent of intertidal area and (3) the sediment import/export to the shelf. Changes to the tidal inundation characteristics, along with being a controlling force in the delivery of sediment to the intertidal and coastal land-building, can also change the distribution of estuarine species, many of which like mangroves occupy depths with specific inundation regimes (e.g. Chen and Twilley 1998).

Methodology

The study began by assessing available data and projected impacts of climate change to determine scenarios for SLR and fluvial discharge that encompassed a likely range of estuarine forcing changes by AD 2115. Field data were collected to calibrate and validate a hydrodynamic model, which were combined with existing sediment data (Felsing and Giles 2011), to also model sediment transport.

Historical data and scenarios

Over the twentieth century (1900–2009), the linear least squares trend in global SLR was $1.7 \pm 0.02 \text{ mm year}^{-1}$ (Church and White 2011). Hannah and Bell (2012) estimated that the average relative SLR trend derived from tide gauges around New Zealand is $1.7 \pm 0.1 \text{ mm year}^{-1}$ over a similar time period. They also determined that the relative SLR trends for the locations closest to Tairua were $1.7 \pm 0.14 \text{ mm year}^{-1}$ at Auckland and $1.9 \pm 0.2 \text{ mm year}^{-1}$ at Moturiki (Mount Maunganui). Vertical uplift rates for the Coromandel Peninsula, including Tairua Estuary, are considered negligible (Kennedy 2008).

For planning and decision timeframes out to the 2090s (2090–2099), based on the Intergovernmental Panel on Climate Change (IPCC) Fourth Assessment reports (AR4), the New Zealand Government recommended a base value SLR of 0.5 m relative to the 1980–1999 average,

accompanied by an assessment of the potential consequences from a range of possible higher SLR scenarios (Ministry for the Environment 2008). At the very least, all assessments should consider the consequences of a mean SLR of at least 0.8 m relative to the 1980–1999 average. Following the release of the IPCC Fifth Assessment reports (AR5), SLR recommendations for New Zealand were revised (Ministry for the Environment 2017). The projected sea levels until AD 2020 for all AR5 scenarios fall within the 0.5–1.2 m range based on the AR4 projections. The exception is an extra H^+ scenario based on the upper tail of RCP8.5 projections, which exceeds 1.2 m in AD 2110. The RCP8.5 H^+ scenario is intended to “stress-test dynamic adaptive pathways, policies and new greenfield and major infrastructure developments” (Ministry for the Environment 2017, p. 105), which is beyond the scope of this study.

The average annual rainfall is 1600–2400 mm year^{-1} at Tairua (Waikato Regional Council 1998). The river flow duration percentiles for the Tairua River at the Broken Hills Station from 2 July 1975 to 1 May 2012 show that 20% of river discharge observations were $< 1.48 \text{ m}^3 \text{ s}^{-1}$, 50% were $< 2.82 \text{ m}^3 \text{ s}^{-1}$ and 80% were $< 6.11 \text{ m}^3 \text{ s}^{-1}$. However, the catchment of the Tairua Estuary can be subjected to heavy rainfall, with maximum 24-h levels recorded along the crest of the Coromandel Peninsula since 1975 ranging from 236 to 426 mm. The maximum discharge recorded at Broken Hills was $9.52 \text{ m}^3 \text{ s}^{-1}$.

For New Zealand, climate change at the end of the twenty-first century is projected to increase westerly winds in winter and spring, resulting in more rainfall in the west of the North and the South Islands and drier conditions to the east and north of the country. Conversely, in summer and autumn, climate models suggest decreased frequency of westerly conditions, with drier conditions in the west of the North Island and a possible increase in rainfall in the Gisborne and Hawke’s Bay regions (Ministry for the Environment 2008). More detailed regional projections were developed by downscaling CMIP5 models (Ministry for the Environment 2018).

For Tairua, the projected impact on rainfall, and hence fluvial discharge, by the end of the twenty-first century is for no change in annual precipitation, but minor seasonal changes of 4–8% consisting predominantly of an increase in winter and a decrease in spring. No change in the frequency of extreme events is expected, which is consistent with a projected decline, or no change, in the frequency of storm events and strength of extreme winds. However, it is also suggested that extra-tropical storms will likely be stronger, with heavy rain and strong winds, which appears to contradict specific rainfall and wind projections. Overall, the projected changes are smaller than the present interannual variability. Although impacts on future rainfall are projected to be minor, the observed discharge of the Tairua River varies from 0.02 to $9.52 \text{ m}^3 \text{ s}^{-1}$.

The present-day conditions and three scenarios of 0.5 m, 0.8 m and 1.2 m SLR for the time period 2010–2115 were used for the modelling, in combination with three scenarios of annual average Tairua River discharge, which can apply to future climate and extreme weather events: $2.5 \text{ m}^3 \text{ s}^{-1}$ (less rainfall or drought), $5 \text{ m}^3 \text{ s}^{-1}$ (no change) and $10 \text{ m}^3 \text{ s}^{-1}$ (higher rainfall or extreme flood).

Field deployment

To provide data for numerical model calibration and validation, two field deployments were undertaken (more details provided in Liu 2014) from 27 July to 4 September 2010 and from 8 June to 11 July 2011 (Fig. 1). Both deployments involved the same instruments at the same locations. Two InterOcean S4ADWs were mounted in fixed frames 0.93 m above the seabed offshore from the Tairua and Pauanui beaches, where they measured water elevation, horizontal current velocities and wave height and period. A SonTek Acoustic Doppler Current Profiler (ADCP) was deployed at the harbour entrance to record water elevation and a profile of horizontal current velocities. Three SonTek Acoustic Doppler Velocity (ADV) current meters were deployed along the main channel of the lower reach of the estuary to measure water elevation and horizontal and vertical current velocities. One RBR tide gauge was deployed in the Tairua River at the SH25 bridge (Hikuai) to record water elevation. Precipitation data were obtained from the Waikato Regional Council (WRC) for the Pinnacles rainfall gauge in the nearby Kauaeranga River catchment (not shown in Fig. 1). Wind data were obtained from the National Institute of Water and Atmospheric Research (NIWA) for the weather station on Slipper Island.

Numerical modelling

Two-dimensional hydrodynamic and sediment transport models (MIKE 21 HD and ST release 2011, Service Pack 6) supplied by DHI Water & Environment were applied in this study (Liu et al. 2011; Liu 2014). MIKE 21 is a numerical modelling system for the simulation of water levels and flows in estuaries, bays and coastal areas. It simulates unsteady two-dimensional flows in single-layer (vertically homogeneous) fluids, using an alternating direction implicit technique to integrate the equations for mass and momentum conservation in the space-time domain. The equation matrices that result for each direction and each individual grid line are resolved by a double-sweep algorithm (DHI 2017).

The bathymetry for the model was derived from LiDAR, multi-beam echo sounder and single-beam echo sounder measurements provided by the WRC and NIWA. Manifold software was used to combine the data and interpolate onto the grids. Median grain size (D50) data provided by the WRC were mapped and showed that D50 ranged mainly from 0.36

to 0.49 mm for the lower reach of the estuary. To reduce the influence of boundary conditions on the interior model domain and to avoid bisecting offshore islands, a large-domain coarse grid ($50 \text{ m} \times 50 \text{ m}$ resolution) that encompasses the entire Tairua Estuary and adjacent shelf area was used. A higher-resolution ($20 \text{ m} \times 20 \text{ m}$) small-domain model, covering only the estuary channel, was nested within the coarse model. The modelling time step was set to 8 s resulting in Courant numbers between 1 and 5.

The model was forced with a time series of tidal elevation, Tairua River discharge and wind velocity. Tidal elevations relative to mean sea level were extracted from NIWA's tidal model every second from 27 July 2010 to 4 September 2010 to provide forcing at the offshore tidal boundaries. Each boundary was interpolated between 20 selected points at 1-min time intervals. Tairua River discharge data were obtained from WRC's Broken Hills Station, which is measured upstream of the maximum tidal influence. Wind velocities were recorded by an Automatic Weather Station on Slipper Island (AWS 31827 B75091, 37.052S 175.943E) maintained by NIWA. The model results were subsequently saved every 75 time steps (10 min).

Calibration of the hydrodynamic model was performed by adjusting the bottom stress as represented by Manning roughness coefficients (Manning number $\text{m}^{1/3} \text{ s}^{-1}$). A uniform Smagorinsky factor of 0.5 (velocity based) was selected as the eddy viscosity for the whole model. The Manning coefficients reflect the median grain size distribution within the estuary: with very coarse to coarse sand in the deeper channels, ranging to fine sand on the upper tidal flats. The initial coefficients estimated from median grain size were adjusted in order to obtain a good overall agreement between observed and modelled water levels and velocities. The final Manning numbers ranged from 32 to $44 \text{ m}^{1/3} \text{ s}^{-1}$, with different values for the intertidal flats, estuary tidal channels and offshore.

The model was then forced with time series data from the second field deployment, and corresponding discharge and wind data from the same sites as for calibration. Modelled tidal elevations and velocities were extracted as close as possible to instrument locations with the estuary and compared with observations (Liu 2014). A statistical analysis of the model fit with observations was performed using the methodologies summarised by Winter (2007) for elevations, and the methodology of Van Rijn et al. (2002) for velocities. The adjusted mean absolute error (AMAE) values for elevation varied over 0.007–0.072 (excellent) within the estuary (Table 1) and 0.042 (excellent) at the SH25 bridge location, which is dominated by fluvial discharge. The relative mean absolute error (RMAE) values ranged from 0.097 to 0.495 (excellent to reasonable). The worst fit was for the ADCP located on the side of the tidal inlet (Table 1), and this is attributed to small-scale tidal eddies not incorporated in the model.

Four models (S1–S4) were run with 0.0, 0.5, 0.8 and 1.2 m SLR, with all other forcings held the same as for calibration

Table 1 Statistics for the fit between measured hydrodynamic conditions and the modelled conditions for the large 50 m × 50 m model and the nested 20 m × 20 m model (in italics)

Instrument	Variable	ME	MSE	RMSE	MAE	RMAE	γ	RMAE (van Rijn)	Qualification
ADP	Water level	−0.008	0.003	0.058	0.046	0.100	0.994	0.17	Reasonable
		<i>−0.009</i>	<i>0.003</i>	<i>0.057</i>	<i>0.046</i>	<i>0.100</i>	<i>0.994</i>	<i>−0.38</i>	<i>Excellent</i>
ADV1	Water level	0.041	0.020	0.141	0.162	0.260	0.944	−2.37	Excellent
		<i>0.007</i>	<i>0.003</i>	<i>0.057</i>	<i>0.044</i>	<i>0.103</i>	<i>0.994</i>	<i>−0.57</i>	<i>Excellent</i>
ADV2	Water level	0.041	0.028	0.166	0.135	0.313	0.948	−2.01	Excellent
		<i>0.011</i>	<i>0.007</i>	<i>0.086</i>	<i>0.069</i>	<i>0.160</i>	<i>0.986</i>	<i>−0.79</i>	<i>Excellent</i>
ADV3	Water level	0.047	0.017	0.129	0.103	0.191	0.965	−1.12	Excellent
		<i>0.030</i>	<i>0.010</i>	<i>0.098</i>	<i>0.074</i>	<i>0.182</i>	<i>0.978</i>	<i>−0.45</i>	<i>Excellent</i>
RBR	Water level	−0.258	0.098	0.313	0.259	0.255	0.990	−0.18	Excellent
		<i>0.058</i>	<i>0.068</i>	<i>0.260</i>	<i>0.163</i>	<i>0.120</i>	<i>0.988</i>	<i>0.04</i>	<i>Excellent</i>
ADP	Current speed	0.064	0.023	0.151	0.115	0.514	0.882	0.29	Good
		<i>0.110</i>	<i>0.031</i>	<i>0.176</i>	<i>0.131</i>	<i>0.588</i>	<i>0.907</i>	<i>0.50</i>	<i>Reasonable</i>
ADV1	Current speed	−0.109	0.035	0.188	0.155	0.318	0.959	−0.23	Excellent
		<i>−0.111</i>	<i>0.028</i>	<i>0.167</i>	<i>0.132</i>	<i>0.272</i>	<i>0.974</i>	<i>−0.23</i>	<i>Excellent</i>
ADV2	Current speed	−0.106	0.030	0.174	0.145	0.400	0.940	−0.29	Excellent
		<i>−0.009</i>	<i>0.013</i>	<i>0.113</i>	<i>0.088</i>	<i>0.244</i>	<i>0.960</i>	<i>−0.03</i>	<i>Excellent</i>
ADV3	Current speed	0.057	0.005	0.073	0.063	0.856	0.940	−0.48	Excellent
		<i>0.057</i>	<i>0.005</i>	<i>0.073</i>	<i>0.063</i>	<i>0.657</i>	<i>0.943</i>	<i>−0.53</i>	<i>Excellent</i>
ADP	Current direction	0.005	0.020	0.143	0.062	0.129	0.965		
		<i>0.038</i>	<i>0.014</i>	<i>0.118</i>	<i>0.059</i>	<i>0.123</i>	<i>0.980</i>		
ADV1	Current direction	0.057	0.023	0.151	0.084	0.230	0.951		
		<i>0.050</i>	<i>0.012</i>	<i>0.111</i>	<i>0.066</i>	<i>0.179</i>	<i>0.975</i>		
ADV2	Current direction	−0.008	0.050	0.224	0.105	0.347	0.844		
		<i>0.111</i>	<i>0.056</i>	<i>0.236</i>	<i>0.186</i>	<i>0.608</i>	<i>0.874</i>		
ADV3	Current direction	−0.288	0.306	0.553	0.391	0.683	0.555		
		<i>0.269</i>	<i>0.202</i>	<i>0.450</i>	<i>0.271</i>	<i>0.476</i>	<i>0.864</i>		

The statistical parameters and qualifications follow the methods of Winter (2007) for elevation and van Rijn et al. (2002) for current speed and direction

and verification. These four models were used to calculate residual currents within Tairua Estuary over 2 consecutive tidal cycles using the MIKE Zero toolbox. To assess how the average sediment transport rate may change with SLR, two-dimensional sediment transport models (MIKE 21 ST) were created based on the hydrodynamic model S1 to S4, and run for 30 model days. The sediment used in sediment transport models was based on the observed grain size and was set to non-cohesive sand with a median diameter of 0.36 mm.

Nine models (S5–S13) were also run with different annual average fluvial discharge scenarios of $2.5 \text{ m}^3 \text{ s}^{-1}$, $5 \text{ m}^3 \text{ s}^{-1}$ and $10 \text{ m}^3 \text{ s}^{-1}$ (i.e. constant discharges) and 0.5 m, 0.8 m and 1.2 m SLR scenarios to study the combined effects of fluvial discharge and SLR.

Results

All model runs indicate that the tidal wave becomes increasingly asymmetrical with distance from the entrance due to

distortion caused by the shallow water depth and friction. Figure 2 shows the progression of changes at each of the instruments from outside the harbour (ADP, top panel) to the most-shoreward deployment (RBR, bottom panel). However, increasing SLR reduced asymmetry and increased tidal range, with the effect becoming greater with distance into the estuary, suggesting that the tidal influence progressed further upstream within the estuary and Tairua River. Relative to run S1 (present sea level), for the S4 run (1.2 m SLR), tidal range progressively increased by 0.012 m (0.66%) at the tidal inlet (ADCP), to 0.286 m (19.28%) at the upstream boundary of the lower estuary (ADV3), and by 0.889 m (107.97%) at the RBR site at the SH5 bridge (Fig. 2, bottom left).

The changing shape of the tidal wave was also reflected in the tidal velocities (Fig. 2, right panels). Increasing SLR results in changing tidal velocities, but the pattern of change differs along the estuary. At the tidal inlet (ADP, top panel), both flood and ebb velocities increase by similar proportions with SLR. In the lower estuary (ADV1 to ADV3), ebb velocities tend to decrease, while flood velocities increase. The

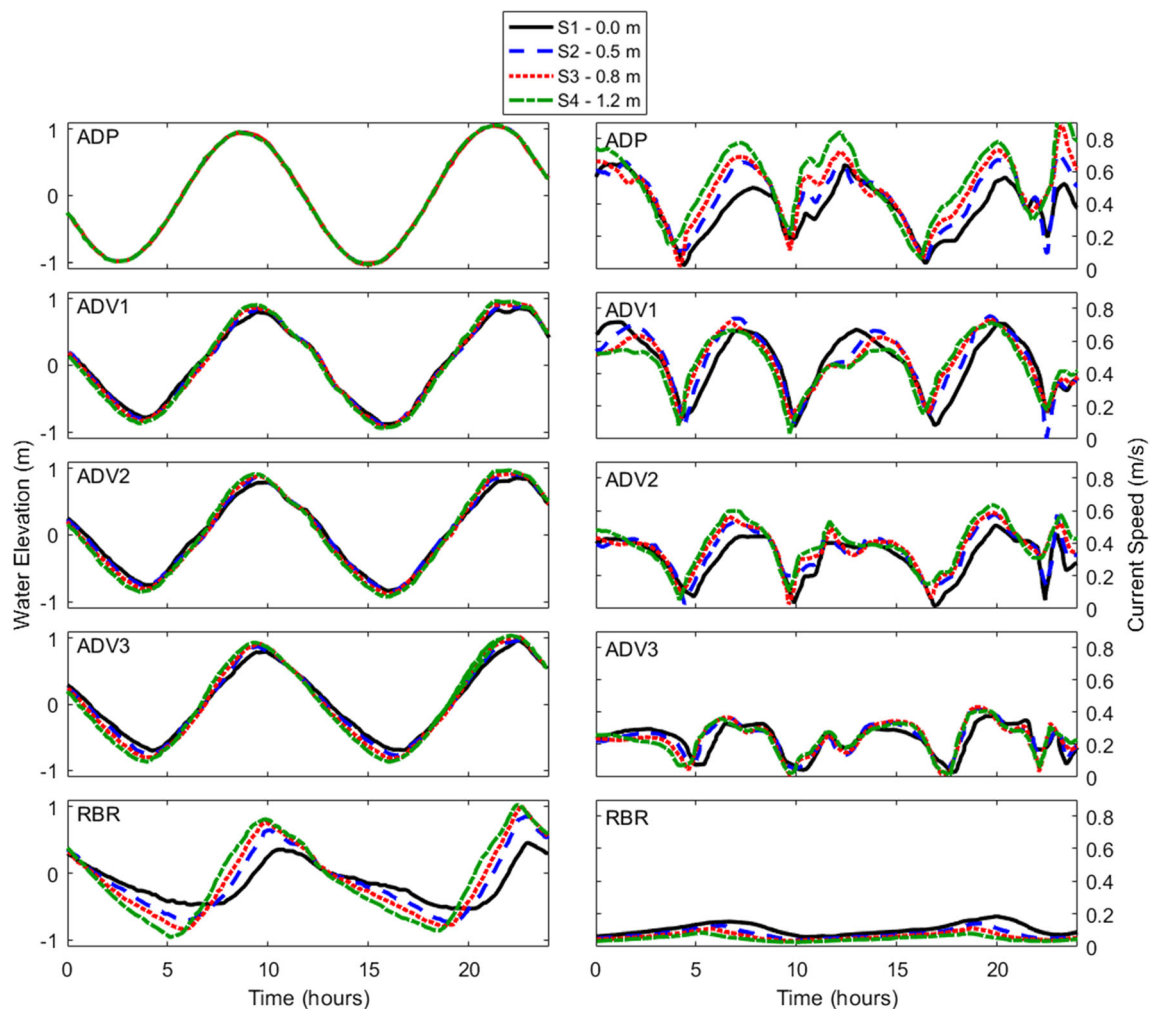


Fig. 2 Predicted tidal elevations (left column) and speeds (right column) at the ADCP, ADV1, ADV2, ADV3 and RBR instrument locations (top to bottom) for different sea level scenarios: S1, 0 m SLR, solid black line;

S2, 0.5 m SLR, dashed blue line; S3, 0.8 m SLR, dotted red line; and S4, 1.2 m SLR, dash-dot green line

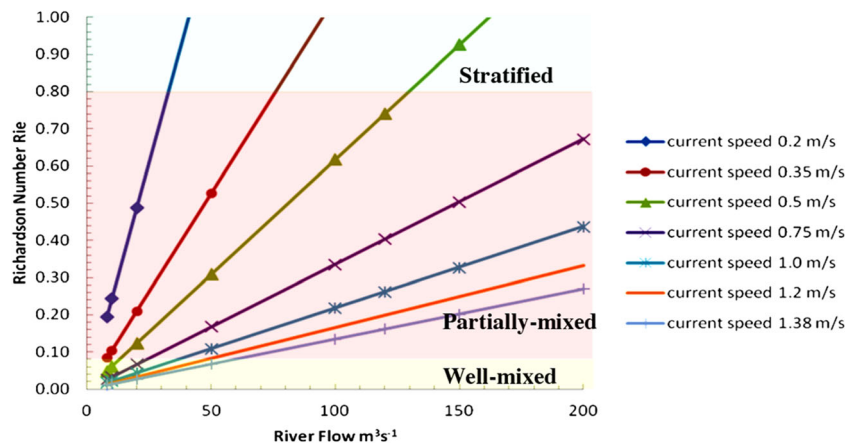
largest ebb decrease occurs at ADV3, while the largest flood increase occurs at ADV2. All sites in the lower estuary (ADP to ADV3) display a change in the phase (timing) of slack water and peak flows.

Changing the fluvial discharge also affected the shoaling behaviour of the tidal wave within the Tairua Estuary, without the effects of SLR (S5–S7) (not shown in Fig. 2). Reduced discharge (2.5 m s^{-1}) decreased the asymmetry of the propagating tide, which was accompanied by an increased tidal range, a reduction in ebb velocities and a slight increase in flood tidal velocities. Increased fluvial discharge (10 m s^{-1}) caused increased asymmetry by increasing the ebb duration, which was associated with increased ebb velocities and reduced flood velocities. Increasing fluvial discharge also changed the density structure of the estuary. Figure 3 shows the changing Richardson number (Ri_E) at the harbour entrance for different tidal current velocities and fluvial discharges. This demonstrates that increasing tidal current velocities drives the estuary towards well-mixed conditions, while

increasing fluvial discharge drives it towards more stratified conditions. CTD data obtained during the second deployment indicated that the estuary became strongly stratified during flood events, so the depth-averaged MIKE 21 HD results may not be realistic for high discharges.

Water surface areas within the estuary were calculated for spring tide during maximum fluvial discharge as an indication of the maximum estuary extent. Areas were determined by counting the number of grid cells covered by water multiplied by the cell area (2500 m^2), and were determined for high and low tides and separately for cells between high and low tides (Fig. 4). With SLR, the spring high tide + flood discharge area increased from 6.4 to 10 km^2 . Due to the hypsometry of the estuary, the low-tide area increased faster than the high-tide area for SLR from 0.8 to 1.2 m , resulting in a reduction in intertidal area for the maximum SLR modelled relative to lower SLR scenarios. Because the tidal range does not change much with SLR (Fig. 2), we expect the tidal prism to scale with area, and so increase linearly.

Fig. 3 Estuarine Richardson number (Ri_E) calculated for the entrance to Tairua Estuary for the range of fluvial discharges and tidal current velocities observed and modelled for the estuary. Average conditions are a fluvial discharge of $9.8 \text{ m}^3 \text{ s}^{-1}$ and tidal current velocity of 0.6 m s^{-1} , corresponding to a partially mixed density structure



The residual currents (Fig. 5) show changing net circulation systems within the estuary as SLR occurs. These currents change in response to the increasing area of the estuary and changing distribution of intertidal and subtidal areas. The key feature as SLR occurs is a decreasing flow concentration within the main tidal channels within the estuary. The added accommodation space means that flow is less likely to be forced into estuarine drainage channels. The residual current analysis did not show any significant changes offshore from the tidal inlet with SLR.

Sediment transport rate (flux) was determined over 30 days of constant tidal forcing for different SLR scenarios. The hydrodynamic conditions were extracted from 1 day (13 August 2010 corresponding to spring tidal range) of the MIKE 21 HD models and repeated to create a 30-day time series. The model results were extracted and scaled to the annual flux ($\text{m}^3 \text{ year}^{-1} \text{ m}^{-1}$) and plotted (Fig. 6). Positive fluxes were defined as seaward sediment transport, and negative fluxes represent landward transport. With increasing SLR, the sediment fluxes within the estuary change from being seaward (sediment export) in the main channels to landward (sediment import). The intertidal areas showed trends of mild increases in sedimentation with increasing SLR.

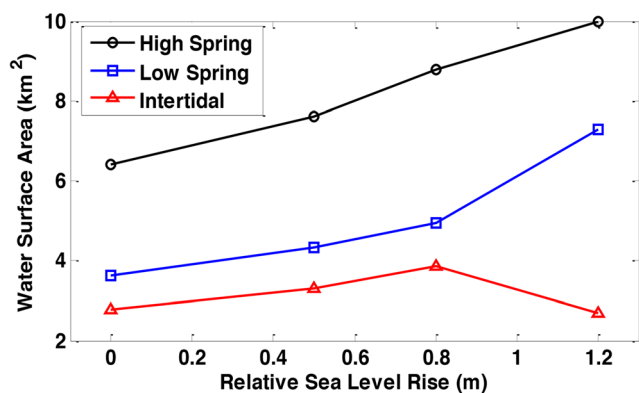


Fig. 4 Thirty-day average water surface areas within the Tairua Estuary during a high tide and low tide, and intertidal area inundated by the tide

Discussion

Increasing SLR effectively rejuvenates the estuary by reversing the general pattern of estuarine evolution (viz. Dalrymple et al. 1992), which involves a shift from importing marine sediment (immature estuary) to exporting fluvial sediment as the estuary infills and evolves towards maturity (Masselink et al. 2011; Carrasco et al. 2016). Our results confirm this, with higher sea level rise causing a reduction in distortion, a shift to reduced ebb dominance and a reduction in the sediment export. Assuming no compensating sedimentation within the estuary, SLR will increase the tidal prism (National Research Council 1987), which should increase tidal velocities given that the tidal duration will not change significantly (Sinha et al. 1997). An increased tidal prism would also change the salinity structure of the estuary by increasing the volume of seawater relative to the freshwater input (Hong and Shen 2012). This assumes that no sedimentation and morphological change occurs, which is likely to not be valid (Carrasco et al. 2016). Morphological models which include sedimentation and the feedback of morphology on hydrodynamics show that morphology adjusts upward to compensate for SLR; the latter is not too extreme (van Maanen et al. 2013). Another response is for the estuary to migrate landward (“roll over”) such as the transgressions that occurred as sea level rose during the Holocene (Townend and Pethick 2002), which depends on whether the coast is protected, and the steepness of the surrounding catchment.

The model results show that increasing SLR results in decreasing distortion of the tide within the estuary. This is associated with an increase in tidal range and a small phase shift, so that low and high tides occur earlier in the tidal cycle. These results are consistent with previous and recent studies (viz. Sinha et al. 1997; Palmer et al. 2019). Increasing fluvial discharge has the opposite effect. Climate projections suggest that future changes to precipitation patterns are minor and less than the current variability. The model results suggest that for the lower SLR scenarios ($\leq 0.8 \text{ m}$), the changes in tidal range

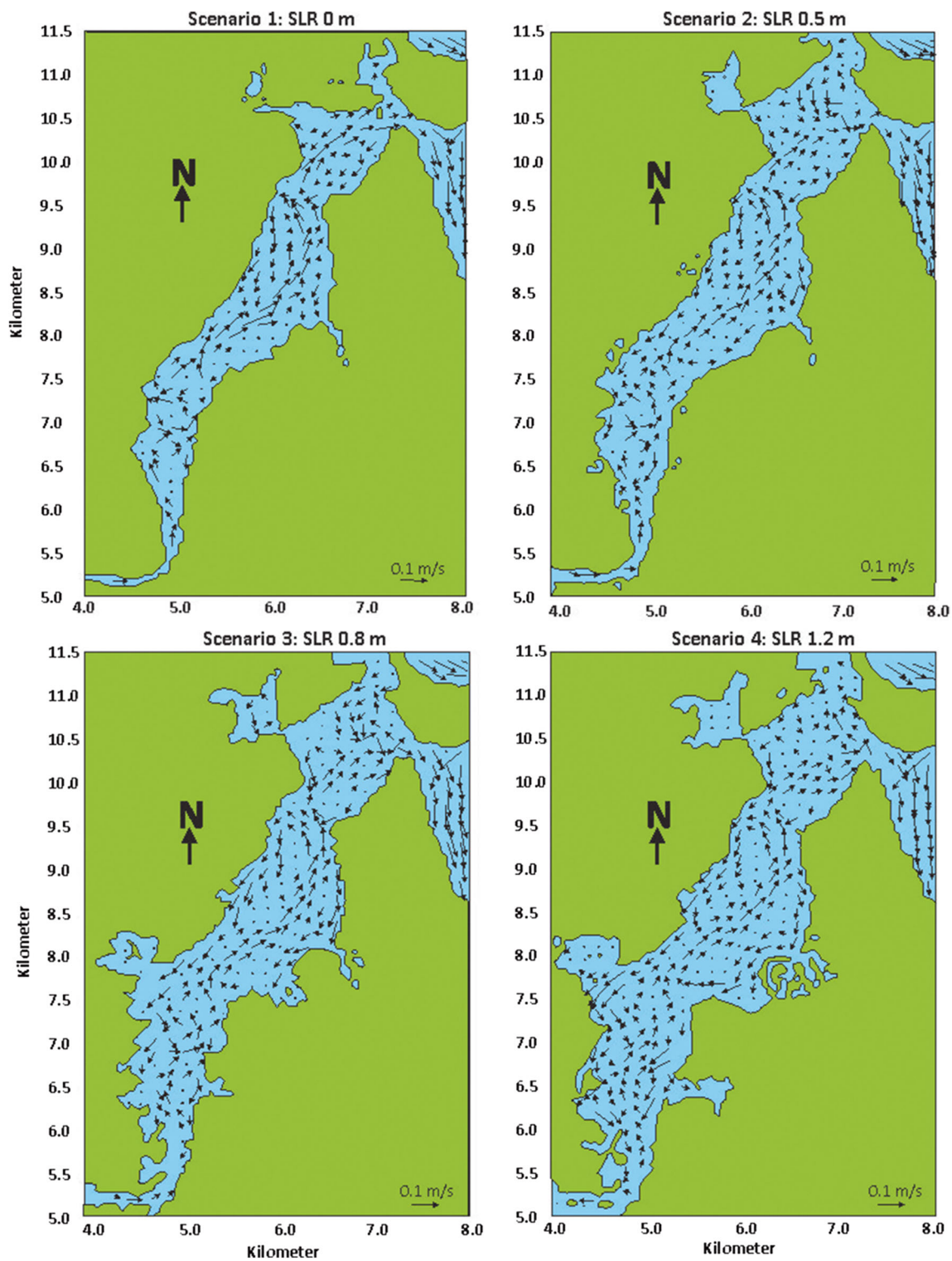


Fig. 5 Residual currents determined over 2 consecutive spring tidal cycles to allow for the diurnal inequality in tidal range present at Tairua. Four SLR scenarios were modelled as discussed in the text, and flood conditions were included to produce the maximum velocities with the estuary

and phase will be within the variation caused by weather-related precipitation variability.

Changing in tidal elevation distributions in response to SLR induces tidal velocity changes, which largely involved

a balancing between flood and ebb velocities as the tides become more symmetrical. The two-dimensional models indicate the largest changes occur in the deeper channels within the estuary. However, the models predicted significant spatial

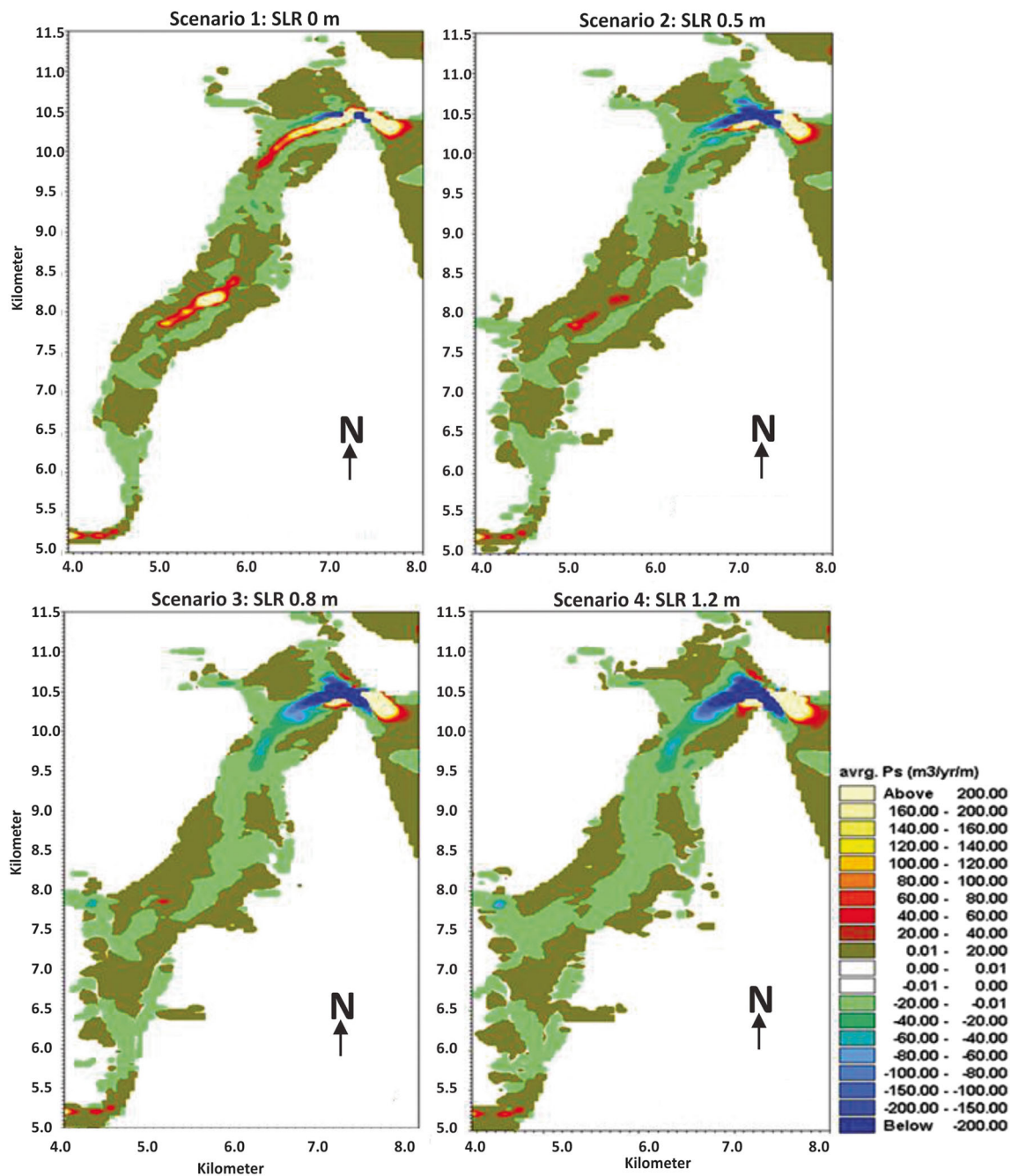


Fig. 6 Annual sediment transport rate derived from an average of the transport rates predicted by 30-day simulations, and scaled up to 365-day totals

variability, even over relatively short lengths of the main tidal/fluvial channel between the Tairua River and the tidal inlet, impacting the residual current circulation within the estuary (Fig. 5). Residual flow plays an important role in the long-term material transport process in the coastal area (viz. Lopes and Dias 2007). The spatial variability highlights the importance of detailed numerical investigations when planning for adaptation for SLR at a specific site.

The intertidal and subtidal surface area within the Tairua Estuary increases with SLR. In our case, the estuary has been allowed to expand by reclaiming new land at its boundaries. In

many more modified catchments, much of the area which could accommodate increasing sea level has been reclaimed by seawalls and stop banks, disrupting the ability of the estuary to respond naturally (Townend and Pethick 2002). Due to variable elevations of the inundated topography, the increase in tidal volume is not a linear function of SLR. Similarly, the change in accommodation space resulting from increased water depth and area inundated with SLR is not a linear function. The model results indicate that accommodation space increases at an accelerating rate for $SLR \leq 0.8$ m, but at a decreasing rate at higher SLR. Implications of the change in

intertidal area are cascading. Species such as mangroves can only tolerate specific inundation regimes and so will need to contract their range to respond to SLR. Recent studies show that light-dependant species such as seagrass rely on exposure to compensate for low light regimes caused by turbid waters (Drylie et al. 2018). Therefore, reduced intertidal extent will increase stress associated with turbidity. Changes to primary productivity can initiate effects on the entire food web.

Modelled sediment transport patterns (Fig. 6) demonstrate that there is a high spatial variation within the estuary. However, some generalisations can be made. With increasing SLR, the main subtidal channels switch from sediment exporting to sediment importing in the lower estuary, whereas the intertidal areas remain as sediment depocentres, although the loci of deposition move in response to residual circulation changes. Ignoring fluvial sediment input, this implies that sediment is likely to be transported from the ebb tidal delta into the estuary. This is evident in the model results, but the modelling did not allow for sediment transfer to the ebb tidal delta from the nearshore along the Pauanui barrier spit. Theoretical morphodynamic models (e.g. Lorenzo-Trueba and Ashton 2014) have suggested that barrier islands respond to sea level rise by changing their geometry (width and height) and migrating landward (also called “roll-over”), which would affect sediment supply to the back barrier lagoon (estuary in the case of Tairua). There are few models that have dynamically coupled the changes to estuaries with the changes to the barriers that enclose them.

If fluvial sediment input is included, the future response will be affected. There are no data for the bedload sediment yield of the Tairua Estuary catchment. Suspended sediment data are recorded for the Broken Hills site on the Tairua River, indicating an average annual yield of 10,842 t of suspended sediment (Hicks et al. 2011). A sediment yield model for the catchment underestimated the measured yield (Hicks et al. 2011), suggesting that the steep catchment and intense rainfall events result in a sediment discharge response that differs from the majority of New Zealand rivers. Although bedload for New Zealand rivers is often estimated as 3% of the suspended sediment, limited data indicates that this is a very unreliable approach (Hicks et al. 2011). Sediment accretion rates within the lower estuary have been measured by Hume and Gibb (1987) for the period 1933–1984, which was linked to an average deposition of $10,000 \pm 2000 \text{ m}^3 \text{ year}^{-1}$ ($\sim 15,300 \text{ t year}^{-1}$ assuming $1 \text{ m}^3 \approx 1.53 \text{ t}$) of sandy sediment. The numerical model results indicate that fluvial discharge is the predominant source of sediment, which is inconsistent with the suspended sediment data but is consistent with the accretion patterns reported by Hume and Gibb (1987).

The vertical accretion rates within the lower estuary ranged from 2 to 22 mm year^{-1} with an average of 6 mm year^{-1}

(Hume and Gibb 1987), which is consistent with the intertidal flat vertical accretion rate of 6.6 mm year^{-1} since European settlement (c. AD 1850) reported for Whangamata Estuary (Sheffield et al. 1995) and for other estuaries around the Coromandel Peninsula (Hunt 2019). If the observed accretion rates continue with ongoing SLR, they are sufficient to mitigate the effects of the 0.5-m SLR scenario as reported for a similar study of the Tamar Estuary in Australia (Palmer et al. 2019), but insufficient for higher scenarios. If the modelled changes in sediment transport patterns occur, the extra sediment supply appears likely to mitigate the effects of the higher scenarios, but with the potential for erosion of the nearshore and beaches of the barrier spit.

Sedimentation responses to SLR will likely lag the increase in accommodation space, rejuvenating the estuary until infilling catches up. This has occurred at least twice before during the Holocene for Tairua Estuary (Clement et al. 2016). These results indicate that better constraints on fluvial bedload contributions to the Tairua Estuary are required to predict the future behaviour of the estuary.

Conclusions

A range of sea level rise projections were combined with fluvial predictions to provide simulations of the hydrodynamic response of an estuary to predicted climate change. Simulations were performed with a calibrated numerical model in Tairua Estuary. In general, the tidal range is expected to increase, and the estuary is expected to shift slowly from ebb-dominant (sediment exporting) to flood-dominant (sediment importing). As long as supply remains sufficient, the increase in imported sediment may compensate for increased accommodation space within the estuary. However, sediment removed from Pauanui Beach might cause an increase in beach erosion. Our modelling results show that responses to SLR, although in general causing a rejuvenating effect on the estuary, vary substantially in space. Detailed modelling investigations are essential when preparing adaptation plans around the New Zealand coast which is complex, due to tectonic processes and a highly variable climate.

Acknowledgements This study was conducted jointly by the University of Waikato and the Waikato Regional Council, New Zealand. Model development was supported by DHI Water & Environment, ASR Marine and Freshwater Consultants Ltd. and MARUM, University of Bremen, Germany. Prof. Christian Winter hosted the INTERCOAST research stay at Marum of Cathy Liu where Cathy set up and calibrated an initial version of the numerical model. NIWA supplied the tidal data for offshore model boundaries. We thank the two anonymous reviewers for their helpful comments.

Funding information Cathy Liu was funded by the Waikato Regional Council and a scholarship from the University of Waikato.

References

- Bell RG (1994) Behaviour of dissolved silica, and estuarine/coastal mixing and exchange processes at Tairua Harbour, New Zealand. *N Z J Mar Freshw Res* 28(1):55–68
- Cahoon DR, Hensel PF, Spencer T, Reed DJ, McKee KL, Saintilan N (2006) Coastal wetland vulnerability to relative sea-level rise: wetland elevation trends and process controls. In: Verhoeven JT, Beltman B, Bobbink R, Whigham DF (eds) *Wetlands and natural resource management. Ecological studies (analysis and synthesis)*, Volume 190. Springer, Berlin, pp 271–292
- Carrasco AR, Ferreira Ó, Roelvink D (2016) Coastal lagoons and rising sea level: a review. *Earth Sci Rev* 154:356–368
- Chen R, Twilley RR (1998) A gap dynamic model of mangrove forest development along gradients of soil salinity and nutrient resources. *J Ecol* 86:37–51
- Church JA, White NJ (2011) Sea-level rise from the late 19th to the early 21st century. *Surv Geophys* 32:585–602
- Clement AJH, Whitehouse PL, Sloss CR (2016) An examination of spatial variability in the timing and magnitude of Holocene relative sea-level changes in the New Zealand archipelago. *Quat Sci Rev* 131:73–101
- Dalrymple RW, Zaitlin BA, Boyd R (1992) Estuarine facies models; conceptual basis and stratigraphic implications. *J Sediment Res* 62:1130–1146
- DHI, 2017, MIKE 21 Flow Model & MIKE 21 Flood Screening Tool, Hydrodynamic Module, Scientific Documentation, 53 pp., http://manuals.mikepoweredbydhi.help/2017/Coast_and_Sea/M21HDFST_Scientific_Doc.pdf
- Drylie TP, Lohrer AM, Needham HR, Bulmer RH, Pilditch CA (2018) Benthic primary production in emerged intertidal habitats provides resilience to high water column. *J Sea Res* 142:101–112
- Felsing M, Giles H (2011) Tairua Estuary shellfish and benthic habitat mapping and assessment of sediment contamination (2009/10), Waikato Regional Council Technical Report 2011/31, Hamilton: Waikato Regional Council, 62 pp.
- Gibb JG, Abum JH (1986) Shoreline fluctuations and an assessment of a coastal hazard zone along Pauanui Beach, Eastern Coromandel Peninsula, New Zealand Water and Soil Technical Publication 27, 48 pp.
- Godoi VA, Bryan KR, Gorman RM (2016) Regional influence of climate patterns on the wave climate of the southwestern Pacific: the New Zealand region. *J Geophys Res Oceans* 121(6):4056–4076
- Hannah, J. and Bell, R. G., 2012. Regional sea level trends in New Zealand, *Journal of Geophysical Research: Oceans*, 117(C01004), <https://doi.org/10.1029/2011JC007591>
- Hayward B, Morley M (2014) Is Coromandel Peninsula rising? *Journal of Auckland Geoclub: Geocene* 11:22–23
- Hemer MA, Church JA, Hunter JR (2010) Variability and trends in the directional wave climate of the Southern Hemisphere. *Int J Climatol* 30(4):475–491
- Hicks DM, Shankar U, McKerchar AI, Basher L, Jessen M, Lynn I, Page M (2011) Suspended sediment yields from New Zealand rivers. *J Hydrol (NZ)* 50(1):81–142
- Hong B, Shen J (2012) Responses of estuarine salinity and transport processes to potential future sea-level rise in the Chesapeake Bay. *Estuar Coast Shelf Sci* 104–105:33–45
- Hume TM, Gibb JG (1987) The “wooden-floor” marker bed—a new method of determining historical sedimentation rates in some New Zealand estuaries. *J Roy Soc New Zeal* 17(1):1–7. <https://doi.org/10.1080/03036758.1987.10421703>
- Hume TM, Herdendorf CE (1988) A geomorphic classification of estuaries and its application to coastal resource management—a New Zealand example. *Ocean Coast Manag* 11:249–274. [https://doi.org/10.1016/0951-8312\(88\)90022-7](https://doi.org/10.1016/0951-8312(88)90022-7)
- Hume TM, Snelder T, Weatherhead M, Liefing R (2007) A controlling factor approach to estuary classification. *Ocean Coast Manag* 50: 905–929
- Hunt S (2019) Summary of historic estuarine sedimentation measurements in the Waikato region and formulation of a historic baseline sedimentation rate Waikato Regional Council Technical Report 2019/18, 30 pp
- Kennedy DM (2008) Recent and future higher sea levels in New Zealand: a review. *NZ Geog* 64:105–116. <https://doi.org/10.1111/j.1745-7939.2008.00132.x>
- Kieft RL, Hampson GJ, Jackson CA-L, Larsen E (2011) Stratigraphic architecture of a net-transgressive marginal- to shallow-marine succession: Upper Almond Formation, Rock Springs Uplift, Wyoming, U.S.A. *J Sediment Res* 81:513–533
- Kirwan ML, Temmerman S, Skeehean EE, Guntenspergen GR, Fagherazzi S (2016) Overestimation of marsh vulnerability to sea level rise. *Nat Clim Chang* 6:253–260
- Liu Z (2014) Hydrodynamic and sediment transport numerical modelling and applications at Tairua Estuary, New Zealand. PhD Thesis, University of Waikato, Hamilton, 306 pp
- Liu C, de Lange W, Winter C, Bryan KR (2011) Forcing mechanisms of a seiche event at Tairua Estuary, New Zealand. In 20th Australasian Coastal and Ocean Engineering conference and the 13th Australasian Port and Harbour Conference (pp. 1–6). Conference held at Perth, Western Australia: EECW Pty Ltd
- Lopes JF, Dias JM (2007) Residual circulation and sediment distribution in the Ria de Aveiro lagoon, Portugal. *J Mar Syst* 68:507–528
- Lorenzo-Trueba J, Ashton AD (2014) Rollover, drowning and discontinuous retreat: distinct modes of barrier response to sea-level rise arising from a simple morphodynamic model. *J Geophys Res: Earth Surf* 119(4):779–801. <https://doi.org/10.1002/2013JF002941>
- Masselink G, Hughes MG, Knight J (2011) Coastal processes and geomorphology. 2nd edn. Hodder Education, London, p 416
- Ministry for the Environment (2008) Coastal hazards and climate change. A guidance manual for local government in New Zealand. 2nd edition. Ministry for the Environment, Wellington, p 127
- Ministry for the Environment (2017) Coastal hazards and climate change: guidance for local government. Ministry for the Environment, Wellington, p 279
- Ministry for the Environment (2018) Climate change projections for New Zealand: atmosphere projections based on simulations from the IPCC fifth assessment, 2nd Edition. Ministry for the Environment, Wellington, p 131
- National Research Council (1987) Responding to changes in sea level: engineering implications. The National Academies Press, Washington, DC, p 160
- Nicholls RJ, Hoozemans FMJ, Marchand M (1999) Increasing flood risk and wetland losses due to global sea-level rise: regional and global analyses. *Glob Environ Chang* 9(1):S69–S97. [https://doi.org/10.1016/S0959-3780\(99\)00019-9](https://doi.org/10.1016/S0959-3780(99)00019-9)
- Palmer K, Watson C, Fischer A (2019) Non-linear interactions between sea-level rise, tides, and geomorphic change in the Tamar Estuary, Australia. *Estuar Coast Shelf Sci* 225
- Sheffield AT, Healy TR, McGlone MS (1995) Infilling rates of a steeppland catchment estuary, Whangamata, New Zealand. *J Coast Res* 11(4):1294–1308
- Sinha PC, Rao YR, Dube SK (1997) Effect of sea-level rise on tidal circulation in the Hooghly Estuary, Bay of Bengal. *Mar Geod* 20(4):341–366
- Smith, R.K., and Bryan, K.R., (2007). Monitoring Beach Volume Using a Combination of Intermittent Profiling and Video Imagery. *Journal of Coastal Research*, 23(4), 892–398. <https://doi.org/10.2112/04-0287.1>
- Townend I, Pethick JS (2002) Estuarine flooding and managed retreat. *Philos T R Soc A* 369(1796):1477–1495. <https://doi.org/10.1098/rsta.2002.1011>

- Van Maanen B, Coco G, Bryan KR, Friedrichs CT (2013) Modelling the morphodynamic response of tidal embayments to sea level rise. *Ocean Dyn* 63(11–12):1249–1262
- Van Rijn LC, Walstra DJR, Grasmeyer B, Sutherland J, Pan S, Sierra JP, (2002) Simulation of nearshore hydrodynamics and morphodynamics on the time scale of storms and seasons using process-based profile models. In: Van Rijn LC (Ed.) *The behaviour of a straight sandy coast on the time scale of storms and seasons: process knowledge and guidelines for coastal management*. March 2002. EC MAST Project, MAS3-CT97-0086, pp. S1–S33.
- Winter C (2007) On the evaluation of sediment transport models in tidal environments. *Sediment Geol* 202(3):562–571. <https://doi.org/10.1016/j.sedgeo.2007.03.019>

Publisher's note Springer Nature remains neutral with regard to jurisdictional claims in published maps and institutional affiliations.